SCIPP 89/30
August 1989
T/E

Beautiful τ Physics in the Charm Land

J.J. GOMEZ-CADENAS

Santa Cruz Institute for Particle Physics
University of California, Santa Cruz, California, 95064

Contribution to the proceedings of the $\tau - Charm$ factory workshop, SLAC, May, 1989

ABSTRACT

The proposed $\tau - Charm\ Factory$ combines several unique features that will make possible to perform very beautiful τ experiments. I will discuss here three examples. The limits on the ν_τ mass, where a sensitivity of the order of 3 MeV can be achieved. The measurement of the one-charged-prong branching fractions, to a fractional error of 0.5-1 %. And the study of the Michel parameters, where precisions comparable to the μ decay experiments can be reached .

1. Introduction

Since its experimental discovery,[1] the τ lepton has been extensively studied. The available data are consistent with the τ being a sequential lepton, forming, together with its neutrino, a "third-generation", Standard Model family.

However, many aspects of the τ physics are not yet well understood. Unlike the lighter leptons, its neutrino has never been observed, and the limit on ν_τ mass is much worse than the limits for ν_e and ν_μ. The V-A structure of its interaction has not been put to a rigorous test yet. The limits on rare decays are much less stringent than in the case of the second-generation lepton, the μ. And little is known about the structure of its massive decays. The reasons for that situation are, first, the relatively poor data sample currently available (the world data set is still of the order of few hundred thousands τ pairs), second, the lack of experimental resolution in past experiments.

The $\tau - Charm\ Factory$ will combine several unique features for τ physics. A state-of-the-art detector, with excellent momentum resolution and particle identification; a machine able to produce *very* large data samples (of the order of 10^7 τ pairs per year); and most important, these τ pairs will be produced at low energy. Although the clean signature of a fast τ (events with one-versus-one or one-versus-trhee back-to-back charged prongs) allows easy and quite efficient selection algorithms, most precision experiments are best performed when the τ is moving slowly. The decay products of a fast-moving τ have higher momentum than those of a τ decaying almost at rest; consequently, the momentum resolution worsens, and particle identification and neutral particle separation become more difficult. On the other hand, the main disadvantage of producing slow moving τ's, the lack of topological separation, can be easily overcome by "tagging" the events. This technique will be discussed several times in the forthcoming sections.

In this paper I will discuss some of the main τ experiments that can be performed in the $\tau - Charm\ Factory$. To illustrate how these experiments can benefit from the possibility of producing low energy τ's, it is interesting to compare our

expected results with those that we project for a *B Factory*. These experiments are also characterized by high rates of τ pairs and excellent detectors, the main difference with a $\tau - Charm\ Factory$ being the energy at which the τ's are produced. Therefore, when comparing results I will assume the same typical rates, and basically the same detector; I will assume however, that a *B Factory* experiment can only take data in the energy range $\sqrt{s} \sim 10\ GeV$.

For this study, I will assume our projected luminosityty of $10^{33}\ cm^{-2}\ s^{-1}$; a "year run" is considered as 5000 hours of data taking. The τ mass is assumed to be $m_\tau = 1.784 \pm 0.3\ GeV$[3] . The detector used in the Montecarlo simulation has been described elsewhere.[2] In Section 2 I discuss the limits on m_{ν_τ}. In Section 3 I discuss the precision measurement of the one-prong-charged branching fractions, $\tau \to e\bar{\nu}_e\nu_\tau$, $\tau \to \mu\bar{\nu}_\mu\nu_\tau$, $\tau^- \to \pi^-\nu_\tau$, and $\tau^- \to K^-\nu_\tau$. Section 4 is devoted to the measurement of the Michel parameters in τ decays. Finally, a brief summary is presented in Section 5.

2. Limits on the τ neutrino mass

The ν_τ, unlike its two closest relatives, the ν_e and ν_μ has not yet been observed. Furthermore, the difficulty of producing a τ neutrino beam, makes the possiblity of detecting interactions mediated by ν_τ remote. The only information that we can extract at present about this particle is provided by the study of τ decays.

The current limit on the mass of the ν_τ[4] $m_{\nu_\tau} < 35$ MeV, is much worse than the limits on the electron neutrino mass[5] $\nu_e < 18$ eV, and the muon neutrino mass[6] $\nu_\mu < 250$ KeV. This limit can be improved up to one order of magnitude by the $\tau - Charm\ Factory$ experiment. The most promising techniques to set a limit on the τ neutrino mass are, the study of the end-point of the energy spectrum of the electron in the leptonic τ decay, $\tau \to e\bar{\nu}_e\nu_\tau$, and the study of the end-point of the invariant mass spectrum of hadronic τ decays to high hadronic-mass final states, such as the decays $\tau^- \to K^-K^+\pi^-\nu_\tau$ and $\tau^- \to \pi^-\pi^+\pi^-\pi^+\pi^-\nu_\tau$. In this section, we will discuss the results that can be obtained with these channels.

2.1. LIMITS ON m_{ν_τ} FROM THE DECAY $\tau \rightarrow e\bar{\nu}_e\nu_\tau$.

The leptonic decay, $\tau \rightarrow e\bar{\nu}_e\nu_\tau$, is, *a priori* a very attractive possibility, since the electron energy distribution can be exactly calculated in lowest order perturbation theory for a massive neutrino, the radiative corrections to this decay are well understood, and the branching fraction is large. To set a limit on m_{ν_τ} one has to study the influence of a massive neutrino on the end-point of the energy distribution. This influence is relatively important if the τ is produced *exactly* at rest, as illustrated in Figure 1, where we show the end-point of the electron energy distribution (x is the electron normalized energy, $x = E_e/E_{max} = 2\ E_e/m_\tau$) for different ν_τ masses. Notice, however, that even in this case a neutrino with a mass below about 10 MeV would be very difficult to detect, since that would require the study of the region $x > 0.9995$, for which a prohibitive resolution in the electron energy, $\Delta E_e/E_e < 0.1\%$, would be required.

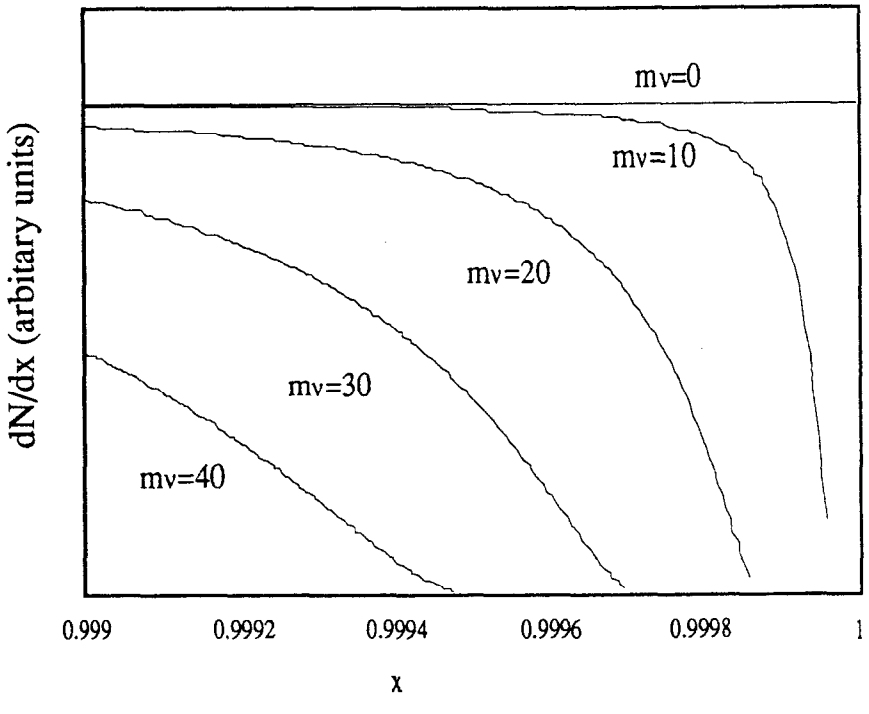

Fig.1 Electron energy distribution ($x > 0.999$) for different m_{ν_τ}; the τ decays at rest.

The situation is in fact worse, since, even taking data right at threshold, the

τ will still be moving with some small momentum due to the beam dispersion ($\Delta E_{beam}/E_{beam} \sim 0.5$ MeV) . Unfortunately, even a small τ momentum changes dramatically the shape and the population of the end-point of the electron energy distribution.

An early study of the possibilities of this channel was done by R.R. Mendel et al.[7]. Further work,[8] showed that the limit on m_{ν_τ} that could be achieved in the $\tau - Charm\ Factory$ was of the order of 20 MeV. However, this limit was obtained assuming that the τ had to be produced with some energy above threshold, since the Born cross section for τ pairs production vanishes when they are produced at rest. On the other hand, the fortunate fact that the corrected τ pair production cross section does not vanish at threshold[11] but approaches a constant value of 0.22 nb (enough to produce several million of τ pairs in one year run) will improve this result, up to an ultimate limit of the order of 15 MeV.

2.2. LIMITS ON m_{ν_τ} FROM THE DECAY $\tau^- \rightarrow K^- K^+ \pi^- \nu_\tau$

The study of the decay $\tau^- \rightarrow K^- K^+ \pi^- \nu_\tau$, opens up a very interesting possibility of improving the limit on m_{ν_τ}. Theoretically, the decay can be well described by a model[10,12] based on the effective Chiral Lagrangian, that also incorporates the effect of the possible resonance structures (the axial part of the current via the A_1 resonance and the vector part via a combination of the ρ and ρ' resonances, together with the $K^* \rightarrow K\ \pi$ system). The differential decay width predicted by the model is

$$d\Gamma \ = \ d\Gamma_{1^+} \ + \ d\Gamma_{1^-} \tag{2.1}$$

where

$$d\Gamma_{1^+} \ = \frac{G_F^2 \cos\theta_c^2}{3^3\ 2^6\ (2\ \pi)^2\ m_\tau\ f_\pi^2}\ \bar{w}(q^2, m_\tau^2, m_{\nu_\tau}^2)\ \lambda^{1/2}(q^2, m_\tau^2, m_{\nu_\tau}^2)$$
$$|F_A(q^2)|^2\ I_{1^+}(q^2)\ \frac{d\ q^2}{q^4}$$

and

$$d\Gamma_{1^-} = \frac{G_F^2 \cos\theta_c^2}{3\ 2^6\ (2\ \pi)^6\ m_\tau\ f_\pi^6}\ \bar{w}(q^2, m_\tau^2, m_{\nu_\tau}^2)\ \lambda^{1/2}(q^2, m_\tau^2, m_{\nu_\tau}^2)$$
$$|F_{1^-}(q^2)|^2\ I_{1^-}(q^2)\ \frac{d\ q^2}{q^4}$$

In the expressions above, $\bar{w}$ is the so-called "weak matrix element"

$$\bar{w}(q^2, m_\tau^2, m_{\nu_\tau}^2) = (m_\tau^2 - q^2)(m_\tau^2 + 2q^2) - m_{\nu_\tau}^2\ (2m_\tau^2 - q^2 - m_{\nu_\tau}^2)$$

while the kinematical function $\lambda^{1/2}(q^2, m_\tau^2, m_{\nu_\tau}^2)$ is defined by

$$\lambda^{1/2}(q^2, m_\tau^2, m_{\nu_\tau}^2) = \{[m_\tau^2 - (\sqrt{q^2} + m_{\nu_\tau})^2]\ [m_\tau^2 - (\sqrt{q^2} - m_{\nu_\tau})^2\}^{1/2} = 2m_{\nu_\tau}|\mathbf{P}_{\nu_\tau}|.$$

The dynamics of the hadronic decay is defined through the functions I_{1^+}, I_{1^-}, F_A and F_1^-. I_{1^+} and I_{1^-} are related with the phase space integral over the hadronic momenta, while F_A and F_{1^-} describe the resonance strucutre. F_A is simply a Breit-Wigner function describing the axial resonance A_1, while F_{1^-} describes the mixing between the ρ and ρ' resonances

$$F_{1^-}(q^2) = [F_{\rho'}(q^2) + \xi\ F_\rho(q^2)]$$

through the mixing parameter ξ. This parameter is estimated to be[10] $\xi \sim -3.2$. In Figure 2, we show the hadronic mass distribution predicted for the model (solid line) and compare it with the distribution obtained for three bodies phase space (dashed line). The predicted branching fractions is 0.4%, consistent with the present experimental value[13] of $0.2 \pm 0.17\%$.

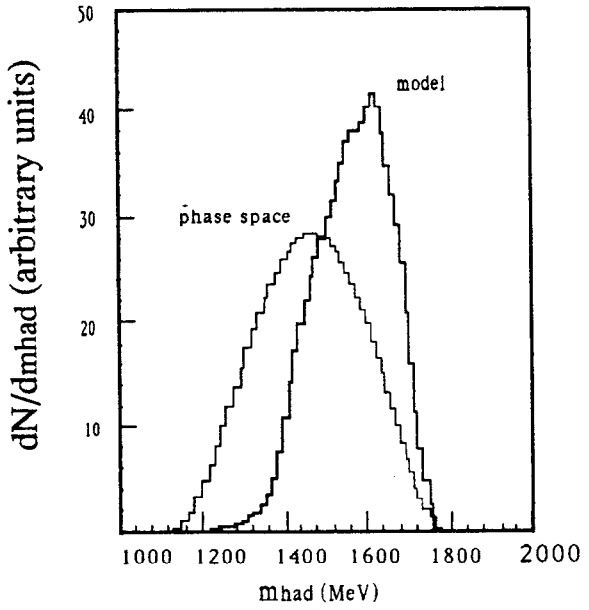

Fig.2 Hadronic mass distribution for the decay $\tau^- \to K^- K^+ \pi^- \nu_\tau$.

Our sensitivity to the τ neutrino mass depends on the behaviour of the hadronic mass distribution close to the end-point. On the other hand, the shape of the hadronic mass distribution near the end-point is completely dominated by the weak matrix element and the kinematical function $\lambda^{1/2}$,and therefore it does not depend on the model. This is illustrated in Figure 3, where we show the end-point of the hadronic mass distribution for our model and for pure 3-body phase space. Notice, however, that our model gives an enhanced population near the end-point of the distribution.

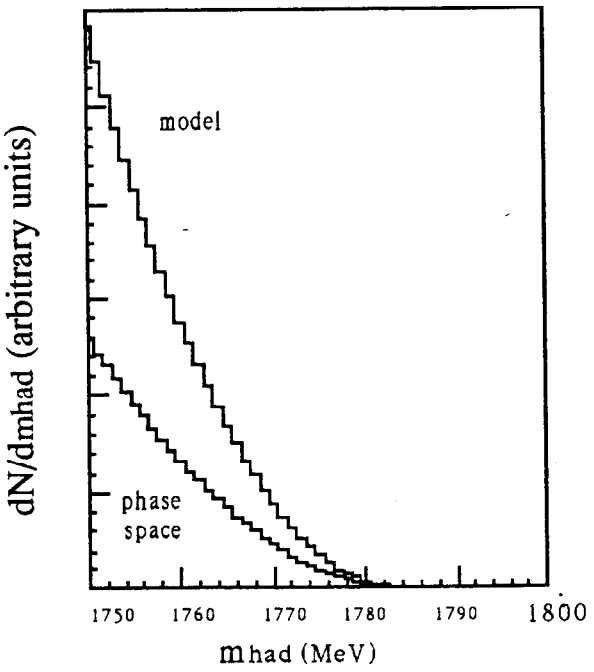

Fig.3 Hadronic mass distribution close to the end-point for the decay $\tau^- \rightarrow K^-K^+\pi^-\nu_\tau$.

For the event selection, we will use one of the τ's as a "tag", accepting only the leptonic channels $\tau \rightarrow e\bar{\nu}_e\nu_\tau$ and $\tau \rightarrow \mu\bar{\nu}_\mu\nu_\tau$. This provides a clean event signature. Exactly four charged tracks in the event, one π and two K's of opposite charge, no neutral energy, a leptonic tag (we impose $P_{lepton} > 400\ MeV$ to guarantee good particle identification) and large missing energy and momentum ($P_{miss} > 400\ MeV$, $E_{miss} > 1\ GeV$). The relevant distributions characterizing the event are shown in figures 4 and 5. The detailed event selection and background suppression has been worked out in Ref. 10, and we illustrate a very similar algorithm in the next section. We find a efficiency for the signal of 30 % with little background.

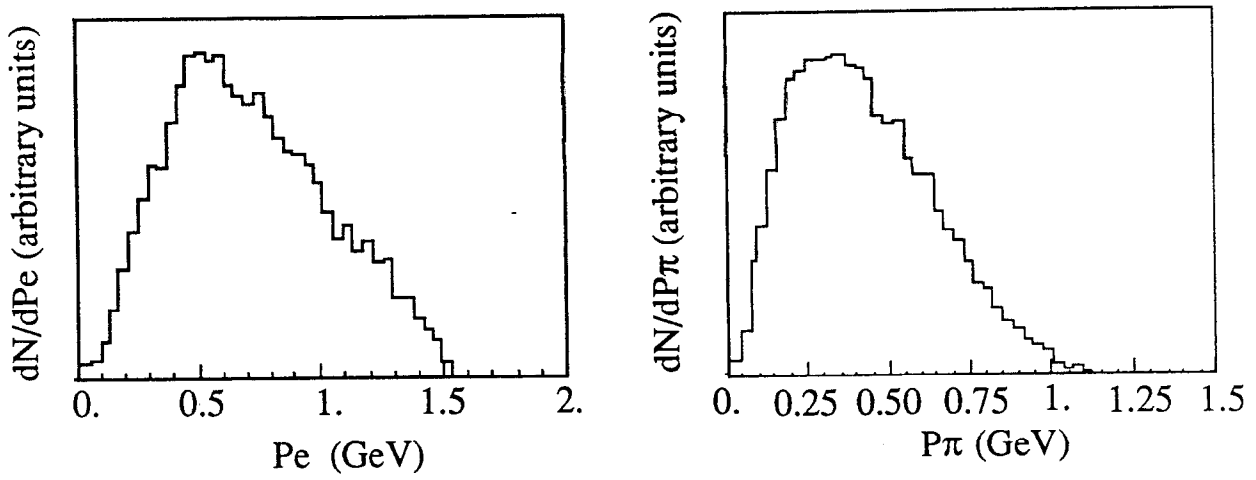

Fig.4 (a) electron energy (b) Inclusive hadron momentum for the decay $\tau^- \rightarrow K^-K^+\pi^-\nu_\tau$.

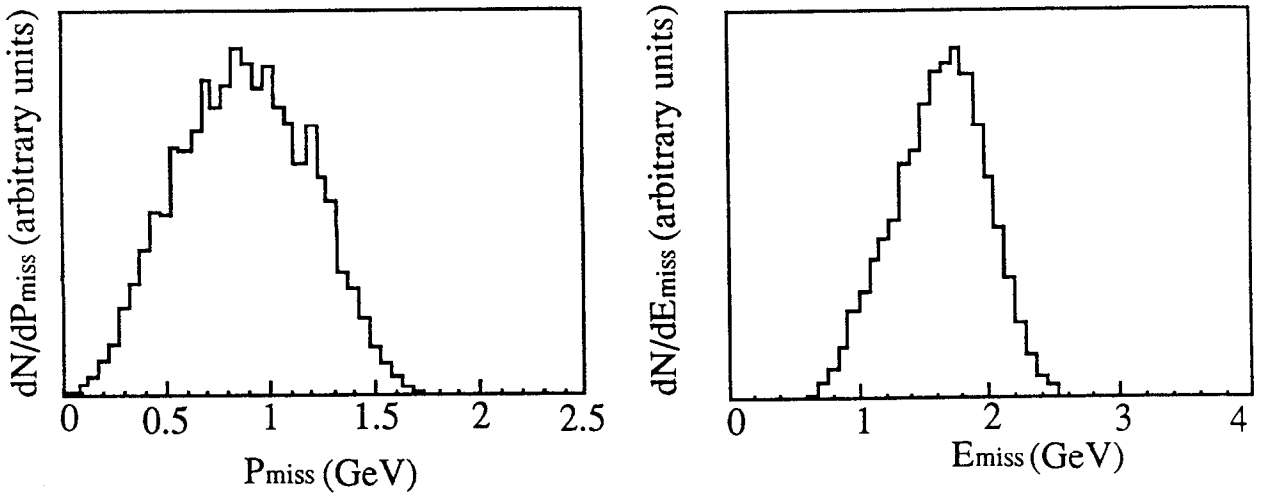

Fig.5 (a) Missing momentum and (b) Missing energy for the decay $\tau^- \rightarrow K^-K^+\pi^-\nu_\tau$.

Unfortunately, the fraction of events with hadronic masses close to the end-point is small, and that will translate in a small data sample for the measurement on m_{ν_τ}. If we perform this experiment at $\sqrt{s} \sim 4.2\ GeV$, near to the peak of the τ pair production cross-section, the number of "useful" events (with $m_{had} > 1750$ MeV) is

$$N_{tagged} \sim 2\, N_{\tau\tau}\, [B(\tau \rightarrow e\bar{\nu}_e\nu_\tau) + B(\tau \rightarrow \mu\bar{\nu}_\mu\nu_\tau)]\, B(\tau^- \rightarrow K^-K^+\pi^-\nu_\tau)\, \epsilon\, \mathrm{f_{end}}$$

where ϵ is the efficiency for detecting the signal, and f_{end} is the fraction of events

(passing all the selection cuts) that have a mass bigger than 1750 MeV. Thus, $N_{tagged} \sim 2 \times 6 \cdot 10^7 \times [0.18 + 0.18] \times 2 \cdot 10^{-3} \times 0.3 \times f_{end} = 2.7 \cdot 10^4 \times f_{end}$;

But $f_{end} \sim 0.36\%$, and therefore, $N_{tagged} \sim 100$ *events/year*. Our sensitivity to m_{ν_τ} is essentially limited by the data sample that we can achieve. We project a limit on m_{ν_τ} of 7 MeV in one year of data taking. That limit improves to 5 MeV in two years.

2.3. LIMITS ON m_{ν_τ} FROM THE DECAY $\tau^- \to \pi^-\pi^+\pi^-\pi^+\pi^-\nu_\tau$.

Unlike the decay $\tau^- \to K^-K^+\pi^-\nu_\tau$, we do not have a good model to describe the dynamics of the decay $\tau^- \to \pi^-\pi^+\pi^-\pi^+\pi^-\nu_\tau$[9]. However, the available experimental data[4], suggests that it must be mediated by a heavy resonance structure. We have considered the simple model in which the decay is assumed to be dominated by the resonance structure $\tau^- \to \rho^0\rho^0\pi^-\nu_\tau$[9] wih the ρ's, subsequently decaying into charged π's. The model provides a mass distribution (See Figure 6) in good agreement with the experimental data (See Ref. 9 for a detailed discussion).

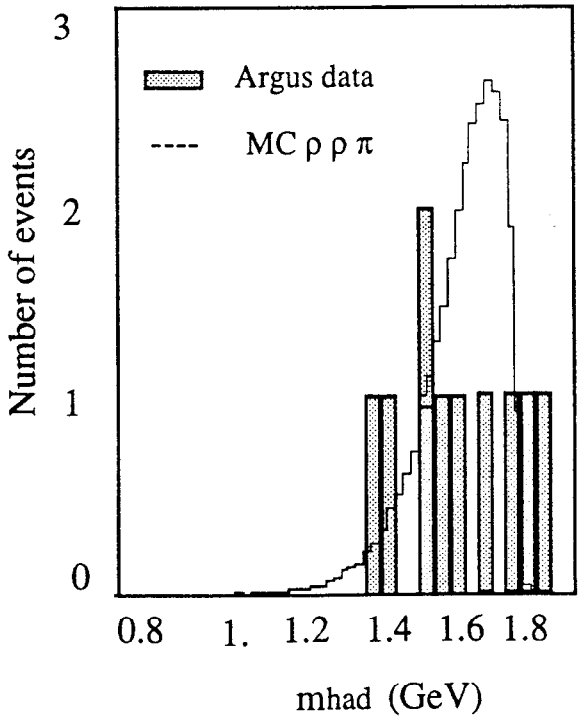

Fig.6 Hadronic mass distribution for the decay $\tau^- \rightarrow \rho^0\rho^0\pi^-\nu_\tau$.

In Ref. 9, we have considered the limits on m_{ν_τ} that can be achieved by studying this decay, taking data at a center of mass energy of $\sqrt{s} = 3.68\ GeV$, below Charm production threshold. The selection algorithm imposes one lepton (again we tag with $\tau \rightarrow e\bar{\nu}_e\nu_\tau$ and $\tau \rightarrow \mu\bar{\nu}_\mu\nu_\tau$) of relatively high momentum ($P_{lepton} > 400\ MeV$), and five, well tracked charged pions; all six tracks must be contained in the detector fiducial volume,$|\cos\theta < 0.9|$, and no neutral energy should be present in the event. In addition , the missing momentum has to be large ($P_{miss} > 400\ MeV$) and the event reduced mass

$$m_{reduced} = \sqrt{(E_{lepton} + E_{miss})^2 - (\mathbf{P_{lepton}} + \mathbf{P_{miss}})^2}$$

must be bigger than the kaon mass. The efficiency for the signal is about 20 %, but the suppression of the hadronic background is extremely good, better than 10^{-6}.

There are several reasons why one can achieve such a good background suppression. First, the fact that the hadronic events have high neutral multiplicity, while the signal event has no neutral tracks. Notice that very hermetic electromagnetic and hadronic calorimeters, with minimum cracks are needed for this selection criteria to be effective. Second, the inclusive lepton momentum spectrum for the hadronic background is peaked at low values, while we require a high momentum lepton. This is illustrated in Figure 7. Third, the missing momentum and reduced mass for the signal are large, unlike the background (see Figure 8.) Finally, the hadronic mass of the background is always large, since at this low energy the multihadron events tend to be very spherical. We illustrate this point in Figure 9.

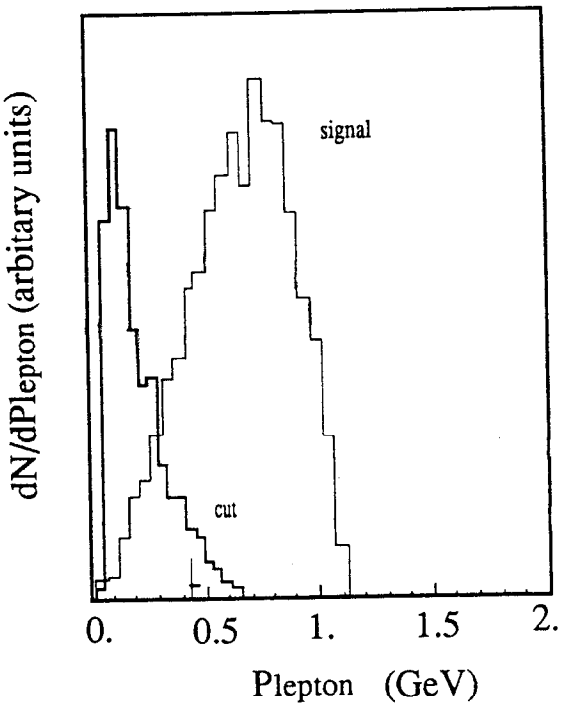

Fig.7 Lepton momentum for the signal and the background.

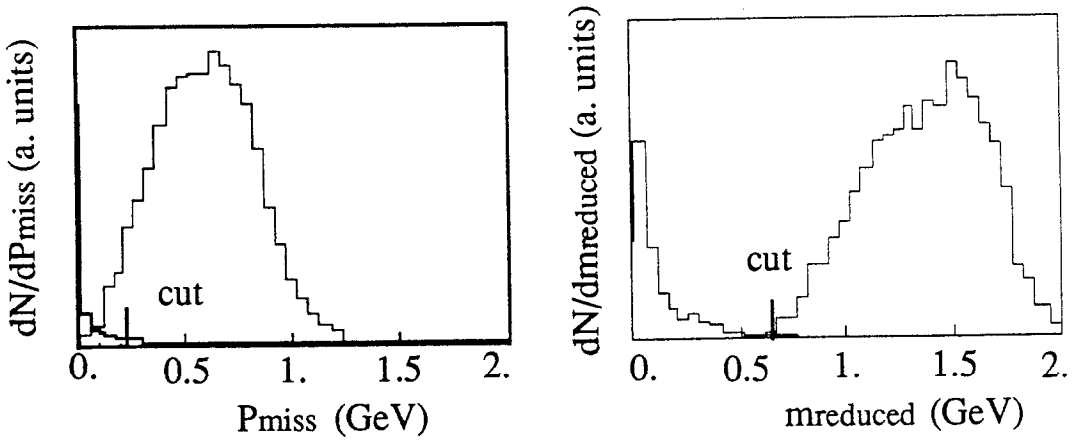

Fig.8 Missing momentum and reduced mass for the signal and the background.

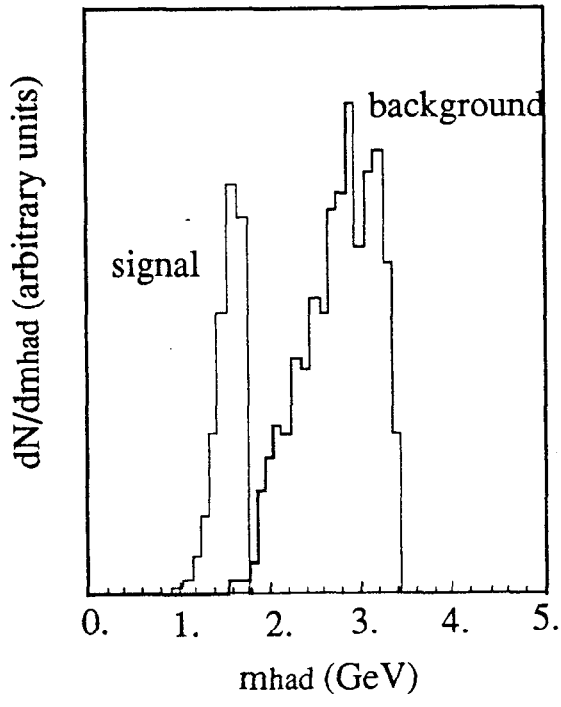

Fig.9 Hadronic mass for the signal and the background.

We obtain that about 350 events per year with a mass $m_{had} > 1750\ MeV$, pass the selection criteria. In Figure 10, we show the hadronic mass distribution for different values of m_{ν_τ}, together with the best fit for them, corresponding to a two year run. In one year we reach a sensitivity of 5 MeV on m_{ν_τ} (90 % C.L.), which is improved to 3.5 MeV in another year of data taking.

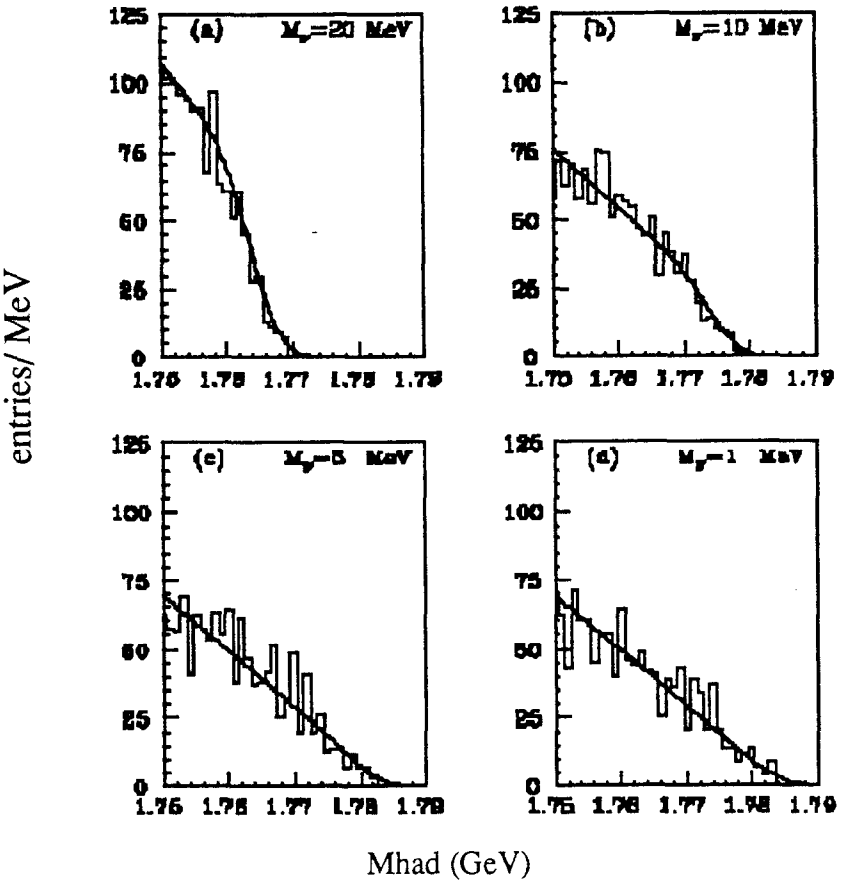

Fig.10 Fits to different neutrino masses for a two year run.

However, we improve this limit somewhat by taking data at 4.2 GeV instead of at 3.68 *GeV*. Besides benefitting from higher statistics, this point has the advantage of allowing a whole set of different experiments to be performed, for instance the study of the spin-spin correlations in τ decays, rare τ decays and several aspects of D physics. The obvious price to pay is to deal with the potential background to the neutrino mass experiment from charmed mesons. To estimate the effect of these backgrounds, we have generated charmed mesons pairs as well as continuum hadron production at 4.2 GeV. Our results are shown in Table-1. According to the simulation, neither any of the exclusive channel that we have studied nor the hadron continuum production is a significant source of background. Thus, the Montecarlo study indicates that the backgrounds to the decay $\tau^- \to \pi^-\pi^+\pi^-\pi^+\pi^-\nu_\tau$ are also

very small at 4.2 GeV. At this energy, we obtain a limit on m_{ν_τ} of 4.2 MeV in one year run, which is reduced to 3 MeV in two year run.

Table 1. Background suppression at 4.2 GeV.

Channel	σ(nb)	Montecarlo sample	fraction of events passing cuts
$D_s\ D_s^*$	0.9	50000	$< 2\ 10^{-5}$
$D_s\ D_s$	0.2	10000	$< 10^{-4}$
$D^*\ D^*$	3.6	100000	$< 10^{-5}$
$D^*\ D$	1.5	50000	$< 2\ 10^{-5}$
$D\ D$	0.2	10000	$< 10^{-4}$
u,d,s (Lund)	12.5	200000	$< 5\ 10^{-6}$
$\tau \to e\bar{\nu}_e\nu_\tau,\ \tau^+ \to \pi^+\pi^-\pi^+\pi^-\pi^+\nu_\tau$	3.5	50000	0.2

2.4. LIMITS ON m_{ν_τ} IN A *B Factory*

Although we will not attempt here a systematic comparation between both type of experiments, there are a few obvious points that can be discussed. First let us consider the leptonic channel, $\tau \to e\bar{\nu}_e\nu_\tau$. This decay channel can only be studied in the $\tau - Charm\ Factory$ experiment. Although the expected improvement in the mass of the τ neutrino is only about a factor 2, it is a necessary cross check of other m_{ν_τ} measurements, since it is theoretically well understood. A *B Factory* experiment, lacking the ability of running *right* at threshold will not be able to extract any useful information about the τ neutrino mass from the study of this channel.

However, the other two decays that we have considered, $\tau^- \to K^-K^+\pi^-\nu_\tau$ and $\tau^- \to \pi^-\pi^+\pi^-\pi^+\pi^-\nu_\tau$, are perfectly valid possibilites. The advantage of the $\tau - Charm\ Factory$ experiment (assuming the same detector), are, first, larger rates (assuming that both machines have the same luminosity), second, better

mass resolution, due to the fact that the τ decay products have lower momentum, and third, better ability to identify particles using conventional techniques. This is illustrated in Figure 11, where we show the inclusive momentum distribution for the decay $\tau^- \rightarrow \pi^-\pi^+\pi^-\pi^+\pi^-\nu_\tau$ at $\sqrt{s} = 4.2$ and 10 GeV. Notice that in the $\tau - Charm\ Factory$ one has to deal only with low energy pions, while in a $B\ Factory$ one needs to worry about both low *and* high energy pions.

To quantify the limits on m_{ν_τ} that can be achieved by both experiments, we can write the empirical formula

$$\sigma_{m_{\nu_\tau}} \propto \frac{\sigma_{mass}}{\sqrt{N}}$$

where $\sigma_{m_{\nu_\tau}}$ is the limit on the ν_τ mass, σ_{mass} is the detector mass resolution, and N is the number of events. In Figure 12, we show the τ cross section as a function of the center-of mass energy. Notice that $\sigma_{\tau\tau}(4.2\ GeV)/\sigma_{\tau\tau}(10\ GeV) = 4$, and therefore, assuming the same luminosity
$\sigma_{m_{\nu_\tau}}(10\ GeV)/\sigma_{m_{\nu_\tau}}(4.2\ GeV) = \sqrt{4}\ \sigma_{mass}(10\ GeV)/\sigma_{mass}(4.2\ GeV)$. If we assume for both experiments our projected momentum resolution

$$[\frac{\sigma_p}{p}]^2 = [0.4\%p(GeV)]^2 + [0.3\%/\beta]^2. \qquad (2.2)$$

We obtain that $\sigma_{mass}(4.2\ GeV) = 2\ MeV$, while $\sigma_{mass}(10\ GeV) = 4\ MeV$. Thus:

$$\sigma_{m_{\nu_\tau}}(10\ GeV)/\sigma_{m_{\nu_\tau}}(4.2\ GeV) = \sqrt{4}\ 2 = 4$$

The worse mass resolution for the $B\ Factory$ is due to the fact that for the high-energy pions ($P_\pi > 1\ GeV$) the first term in equation (2.2) is not negligible.

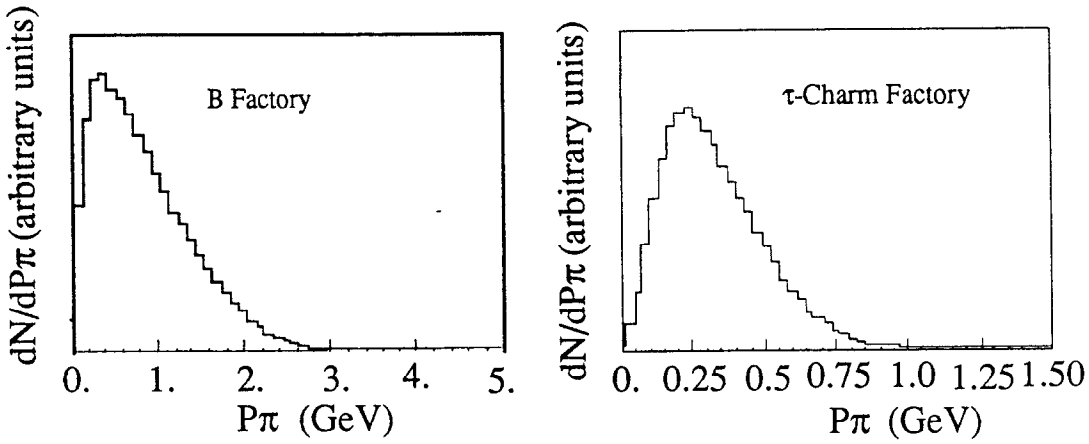

Fig.11 Inclusive momentum distribution for the decay $\tau^- \to \pi^-\pi^+\pi^-\pi^+\pi^-\nu_\tau$ at $\sqrt{s} = 4.2,\ 10\ GeV$.

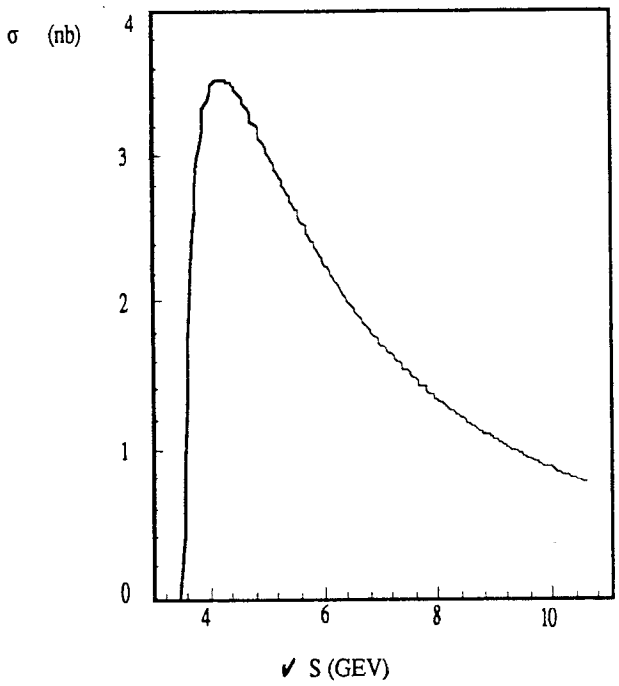

Fig.12 The τ pair cross section as a function of $\sqrt{s}$.

Therefore, if we assume the same luminosity, we obtain that the limit on m_{ν_τ} that a *B Factory* can achieve is a factor 4 worse than the one that can be achieved by a $\tau - Charm\ Factory$. If we assume a greater luminosity for the *B Factory* so that both experiments can collect similar data samples, the difference is still a factor two.

Finally, both experiments will need a very careful understanding of the backgrounds. The ability of the $\tau - Charm\ Factory$ of taking data both below charm production threshold *and* below τ production threshold will be important here, since it will allow a background study that is not based only in Monte Carlo simulation.

3. Precision measurement of the one charged prong branching fractions

The precision measurement of the branching fractions B_e, B_μ, B_π, and B_K for the processes $\tau \rightarrow e\bar{\nu}_e\nu_\tau, \tau \rightarrow \mu\bar{\nu}_\mu\nu_\tau, \tau^- \rightarrow \pi^-\nu_\tau$, and $\tau^- \rightarrow K^-\nu_\tau$ is perhaps, the most elegant τ experiment that the $\tau - Charm\ Factory$ can perform. The partial widths for these decays are accurately calculated within the context of the Standard Model. The present experimental values agree with the theory predictions, but the experimental errors (particularly in the case of the hadronic decays $\tau^- \rightarrow \pi^-\nu_\tau$ and $\tau^- \rightarrow K^-\nu_\tau$) are much larger than the fine predictions of the theory, namely the radiatively corrected values for the decay widths. This is illustrated in Table-2. Notice that the radiative corrections to the hadronic decay widths are of the order of 1 %, a much smaller effect than the experimental error (6 % for $\tau^- \rightarrow \pi^-\nu_\tau$, 30 % for $\tau^- \rightarrow K^-\nu_\tau$).

Table 2. Ratio of Branching Ratios for Accurately Predicted τ decays

Ratio	Present values	Theory (No Rad. Corr.[14])	Theory (Rad. Corr.[15])
μ/e	1.02 ± 0.03	0.973	0.973
π/e	0.62 ± 0.04	0.607	0.601
K/e	0.038 ± 0.011	0.0395	0.0399

Therefore, a precision on the one charged prong branching fractions of the order of 1% is needed only to be able to precisely-test the theory. In addition,

there are a number of "New Physics" scenarios[16,17] that can lead to deviations from the expected values. Also, it has been pointed out[18,19] that the precision measurement of the branching fraction B_e to the 1% level could yield an indirect measuement of Λ_{QCD} to a precision of 25 MeV, thus reducing the present error by a factor four.

To measure B_e, B_μ, B_π and B_K to the one percent precision level one needs not only a large data sample, but also to keep the systematic errors at this level. There are two main requirements to achieve this goal. First, the technique to unfold the branching fractions has to depend as little as possible of the detector simulation, and second, the particle confusion has to be minimum. The $\tau - Charm\ Factory$ experiment can meet both requirements thanks to the possibility of taking data at threshold.

Taking data just above trheshold, (i.e. at $\sqrt{s} = 3.57\ GeV$) adds an additional, extremely powerful particle identification technique to the detector capabilities. The τ is produced almost at rest, and therefore, the π and K emitted in the decays $\tau^- \rightarrow \pi^-\nu_\tau$ and $\tau^- \rightarrow K^-\nu_\tau$ are quasi-monochromatic. Thus, the π and K momentum spectra are narrow spikes at 890 and 820 MeV respectively. This is illustrated in Figure 13 and 14, where we show the momentum spectra for the e,μ, π and K at$\sqrt{s} = 3.57\ GeV$, (just 1 MeV above τ threshold) and at $\sqrt{s}\ = 4.2\ GeV$, close to the peak of the cross section. Notice, that, while in the second case all the particles are mixed together, near threshold they separate almost perfectly. The π and K spectra do not overlap, and the overlap between the electron (μ's) and π's and K's is, small; in addition, at this energy range we can separate e/μ/π and e/μ/K by several techniques. Electromagnetic and hadronic calorimetry, muon range, and dE/dx and TOF.

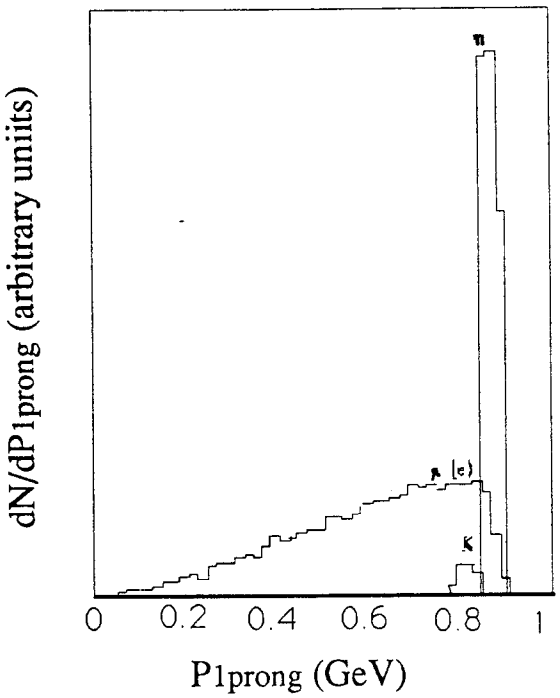

Fig. 13 Momentum spectra for the τ decays to e,μ, π and K ($\sqrt{s} = 3.57\ GeV$).

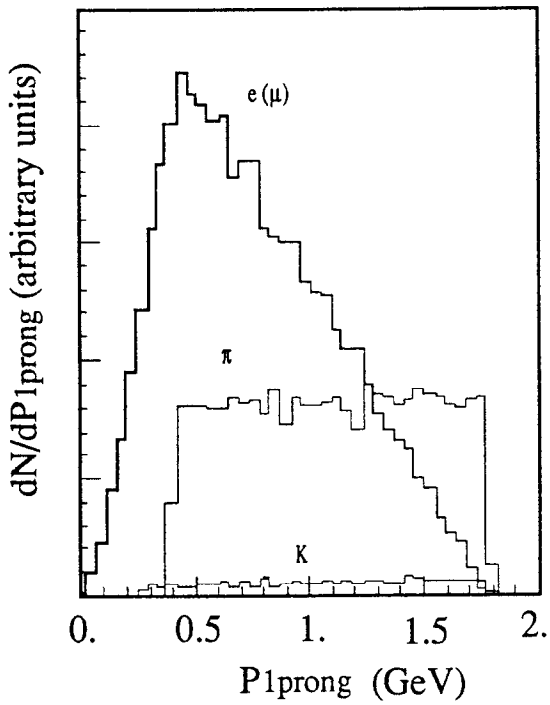

Fig.14 Momentum spectra for the τ decays to e,μ, π and K ($\sqrt{s} = 4.2\ GeV$).

To measure the one prong branching fractions we will use the decay $\tau^- \rightarrow \pi^- \nu_\tau$ as a tag; we then use the decay of the other τ to compute the branching fractions. Thus, we select events with only two charged tracks and no neutrals; one of the tracks has to be a π; the other, either an electron, μ or K. For that experiment, we call a particle an electron if its momentum is less than 860 MeV (thus avoiding $\pi - e$ confusion); if the TOF and dE/dx measurements are electron-compatible, and the energy deposition and shower profile in the calorimeters are compatible with the electron hypothesis. We call it a μ if its momentum is less than 860 MeV, if TOF and dE/dx make it muon-compatible, if it behaves like a minimum-ionazing particle in the electromagnetic calorimeter, and penetrates with the correct range in the hadronic calorimeter. The particle is called a π if its momentum is greater than 860 MeV and is not compatible with the electron and muon hypothesis. Finally, we call the particle a K if its momentum range is $780 < P_K < 860\ MeV$, and is compatible neither with an electron nor with a μ. In Table 3 we show the level of separation that can be achieved between e,μ,π, and K, with these criteria, together with the techniques relevant for their separation.

Table 3. Particle Separation at Threshold

particles	Confusion level	Energy Range	Separation Technique
$e - \mu$	$< 10^{-3}$	$P_e,\ P_\mu > 100\ MeV$	dE/dx,Calorimetry,TOF
$e - \pi$	$< 10^{-6}$	$P_e < 860\ MeV$	dE/dx,Calorimetry, Kinematics
$e - K$	$< 10^{-5}$	$P_e < 860\ MeV$	dE/dx,Calorimetry, TOF, Kinematics
$\mu - \pi$	$< 10^{-6}$	$P_\mu < 860\ MeV$	Calorimetry,Kinematics
$\mu - K$	$< 10^{-4}$	$P_\mu < 860\ MeV$	Calorimetry, TOF, Kinematics
$\pi - K$	$< 10^{-6}$	$P_K < 860\ MeV$	TOF, Kinematics

To measure the branching fractions, the first step is to determine B_π in a fashion that does not depend of our knowledge of the total number of τ pairs produced, $N_{\tau\tau}$. To do this, we proceed as follows

i) Select events where both τ's decay via $\tau^- \rightarrow \pi^- \nu_\tau$. These are extremely clean, virtually background-free events. Fitting the obtained distribution, we establish the π spectrum. The number of events where both τ's decay via $\tau^- \rightarrow \pi^- \nu_\tau$ is

$$N_{\pi\pi} = N_{\tau\tau}\ B_\pi^2$$

ii) Determine the number of events where one τ decays via $\tau^- \rightarrow \pi^- \nu_\tau$ and the other decays to anything

$$N_\pi = 2\ N_{\tau\tau}\ B_\pi$$

The signal in this case is not as obvious as above. Still, our event selection must be able to supress the hadronic background, while keeping the efficiency close to 100 % for the τ's, otherwise we will introduce a systematic error that will spoil our determination of B_π.

A priori, this looks like a difficult exercise, since, due to the low τ pair production cross section at threshold, the ratio signal to background is very high, $\sigma_{had}/\sigma_{\tau\tau} \sim$ 50. Fortunately, the signal is characterized by several distinctive features. The ν_τ produced in the decay $\tau^- \rightarrow \pi^- \nu_\tau$ has the same energy as the detected π, thus the missing energy in the event is very large. The other τ decays practically 100 % of the time to either one or three charged prongs. In addition, we know that Baryons are not produced in τ decays, and the number of neutral mesons (other than π^0) produced is negligible. Then, we impose the following cuts: missing energy in the event larger than 800 MeV, only 2 or 4 charged tracks, and no protons or neutral hadronic energy detected.

In Figure 15 we illustrate how the missing energy cut reduces the background. With these criteria the hadronic background is reduced by a factor 25 while keeping practically 100 % of the τ's. In Figure 16, we show the signal and background distributions after the cuts. The ratio signal to background in the π peak region is 3 to 1.

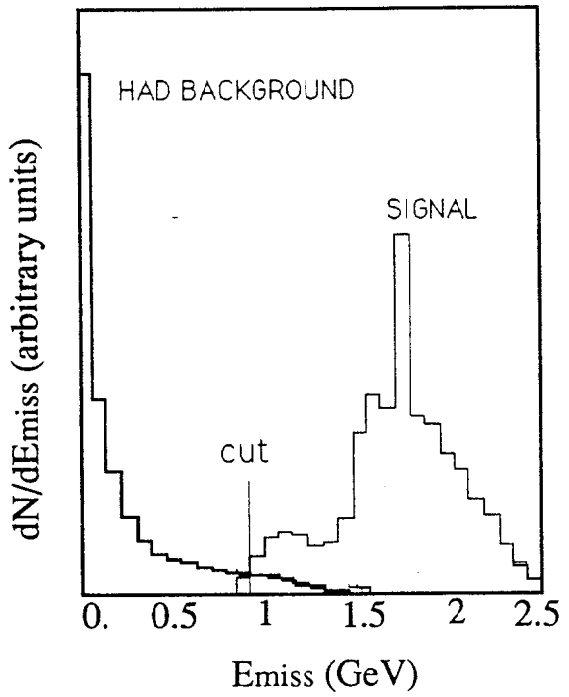

Fig. 15 Missing energy for the signal and the hadronic background.

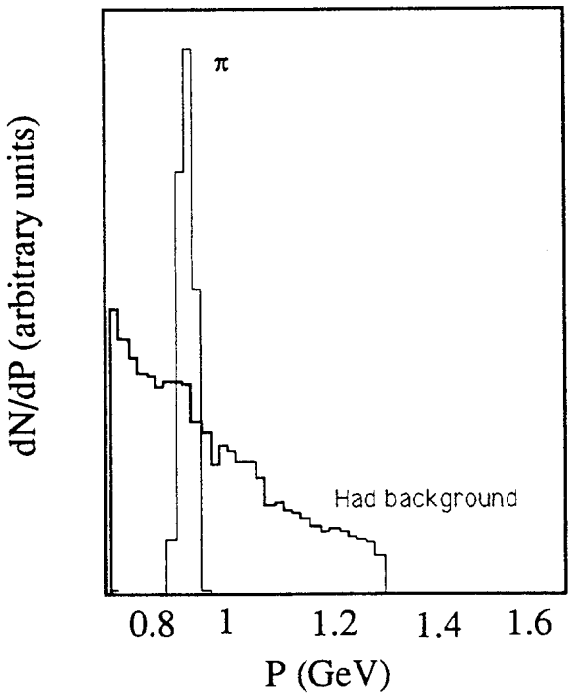

Fig. 16 The signal and the hadronic backgrounds after the selection cuts.

The last step is to fit the shape that we have previously determined for the π spectrum, letting only one free parameter that describes the background. The fit will provide N_π.

iii) Once determined $N_{\pi\pi}$ and N_π, B_π is obtained by simply dividing these two quantities. The error on B_π is very small. In a few months of taking data we obtain typical rates of $5 \cdot 10^5$ single π decays and $2.5 \cdot 10^4$ double π decays. This yields a fractional error on B_π smaller than 0.4 %.

Once we have determined the normalizing branching fraction B_π the other one prong branching fractions are easily obtained using a conventional unfolding technique. We select $e - \pi, \mu - \pi$ and $K - \pi$ pairs. Then we measure $N_{i\pi}$, the number of events of the type i(i=e, μ, K) tagged by a π. The branching fraction for this channel, B_i is, ignoring particle confusion

$$B_i = \frac{N_{i\pi}}{N_\pi}.$$

To take into account the small particle confusion we compute an efficiency matrix ϵ_{ij} that describes the probability of detecting a τ that decayed via the the channel i in the topology j. The number of events observed in a given topology $N_{i\pi}$, are Poisson distributed around the expected number of events $M_{i\pi}$ in this category. Then, we have

$$B_i = \frac{\epsilon_{ij}\ M_j}{N_\pi}.$$

The systematic error here is introduced by the necessity of estimating ϵ_{ij} by Montecarlo simulation. However, the particle confusion is very small, and thus, the systematic error introduced by this estimation is also very small, less than our statistical errors. The efficiency matrix ϵ_{ij} is indeed, practically diagonal.

Finally we construct the Poisson distribution for our set of branching fractions.

$$L = \prod_i \frac{M_i^{N_i}\ e^{-M_i}}{N_i!}$$

and find the set of branching fractions that maximizes the Likelihood function L

(actually, we minimize $-\log L$).

With this technique we obtain B_e, B_μ and B_π with a fractional error of 0.4%. B_K is obtained with less precision, $B_K = 3\%$, since the kaon data sample obtained with the π tag is much smaller than the data samples for electrons and muons. However, this result can be improved. Once we have measured B_e, B_μ to the 0.4 % precision, we can now select $e - K, \mu - K$ pairs and redetermine B_K with a data sample five times bigger. This will yield the measurement of B_K with a 1 % fractional error.

In conclusion, the $\tau - Charm\ Factory$ experiment will be able to measure the one prong branching fractions to a precision level sufficient to test the radiative corrections of the theory. As discussed, this impressive result is only possible because of our ability of combining a large data sample with the kinematical separation provided by running at threshold. These two conditions cannot be met by any other experiment.

4. Study of the Weak current structure in leptonic τ decays

One of the less well established properties of the τ lepton is the structure of the weak current that mediates its decay. In order to determine the structure of the weak current it is necessary[20] to measure the following observables.

i) Lifetime.

ii) Decay asymmetry of the daughter lepton (μ or e) relative to the spin of the τ, described by the parameters ξ and δ.

iii) Polarization ξ' of the daughter lepton.

iv) Total cross section for the inverse decay $\nu_\tau e^- \rightarrow \tau^- \nu_e$ with ν_τ of known helicity.

While all these quantities have been measured for μ decays, only the lifetime has been measured for τ decays. Furthermore, the experiment measuring the reaction

$\nu_\tau e^- \rightarrow \tau^- \nu_e$ is hardly conceivable at present, due to the difficulty of generating a ν_τ beam.

Another quantity that gives information on the nature of the weak current is the so-called Michel parameter ρ. Although a precise determination of the above quantities would fix its value automatically, a direct measurement of ρ is nevertheless very interesting, specially in the case of τ decays where there are no prospects of performing a "ν_τ scattering" experiments. The Michel parameter has been measured to agree with the expected "V-A" value of 3/4 to within 10 %. In contrast, the experimental error on ρ for the μ decay is 0.3 %, almost two orders of magnitude smaller. No measurement exists for τ decays of the low part of the energy spectrum, described by an additional parameter, η.

The implications of the precise measurements of these parameters have been discussed elsewhere[21,22,23]. See also Ref 21, and 24, for a discussion of the relation between the Michel parameters and the most-general, derivative-free, four-fermion Hamiltonian, describing the structure of the weak current in leptonic τ decays. Here we will only make a few points.

i) The structure of the weak current is determined *almost* completely by measuring the Michel parameters ρ, η, δ, ξ, and ξ', together with the τ lifetime. There is a remaining ambiguity that cannot be solved without a "neutrino scattering" experiment $\nu_\tau\ e^- \rightarrow \tau^- \nu_e$. If all these parameters are found to have "V-A" values, the interaction can still be an arbitrary mixture of V-A and scalar couplings.

ii) A "V-A" value for the Michel parameter, $\rho = 3/4$ implies only that there is no "chirality changing" vector and tensor currents present in the interaction. It does not exclude some of the most obvious "New Physics" phenomena, such as right handed bosons or charged Higgs scalars. However, if an upper or a lower limit, $\rho < 3/4$ or $\rho > 3/4$ is found, then some kind of new interaction must be present. Due to the large experimental error on the current value of ρ there could be a large mixture of new interactions not excluded by the current

experimental value of ρ. A very precise measurement of ρ_e, ρ_μ would be of importance to investigate the possible presence of these new interactions.

iii) The parameters ξ, δ and ξ' have not yet been measured in τ decay. However, unlike ρ, they are very sensitive to the presence of strongly coupled charged Higgs scalars and right handed bosons. Measurements of these quantities will yield limits on the masses of these particles.

4.1. MEASUREMENT OF ρ IN THE $\tau - Charm\ Factory$

Consider the leptonic decay $\tau \rightarrow l\bar{\nu}_l\nu_\tau$. The energy spectrum of the emitted lepton in the τ rest frame is given by:

$$\frac{dN}{dx} = N_0 \cdot x^2 G(x,\rho) \tag{4.1}$$

where N_0 is a normalization constant and

$$G(x,\rho) = 1 - x + \frac{2}{3}\rho(\frac{4}{3}x - 1)$$

and $x = E_l/E_{max} = 2E_l/m_\tau$. In Figure 17, we show the emitted lepton energy spectrum for two different values of ρ.

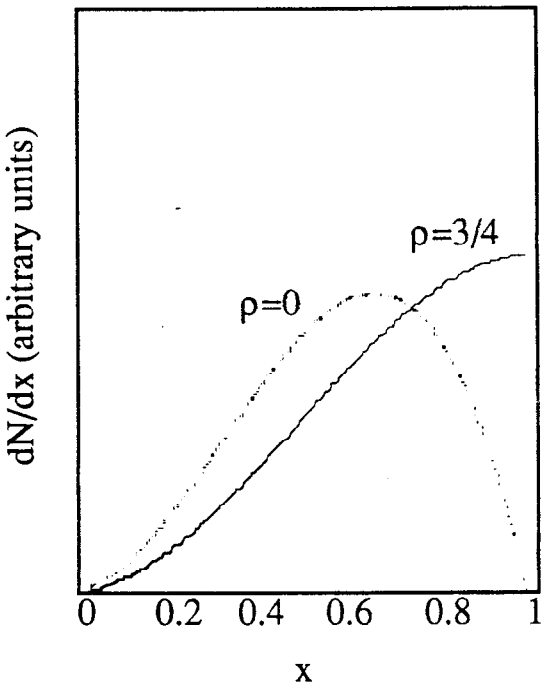

Fig. 17 E_{lepton} for the decay$\tau \rightarrow l\bar{\nu}_l\nu_\tau$ in the τ rest frame

In the laboratory frame, where the τ is moving with velocity β we can write (assuming negligible masses for all the τ decay products)

$$\frac{dN}{dx} = N_0[1 - c(E_\tau)x + \frac{2}{3}\rho(\frac{4}{3}c(E_\tau)x - 1)] \text{ for } x < x_c \tag{4.2}$$

$$\frac{dN}{dx} = N_0[3(1 - 3x^2 + 2x^3) + \frac{2}{3}\rho(-1 + 9x^2 - 8x^3)] \text{ for } x > x_c$$

with

$$c(E_\tau) = \frac{3E_\tau^2 + P_\tau^2}{3E_\tau(E_\tau - P_\tau)}; \quad x_c = \frac{1-\beta}{1+\beta}.$$

In Fig. 18, we show the energy distributions dN/dx for different values of the center of mass energy. Notice that the shape of the distributions depends strongly on β, changing from an increasing polynomial for $x < x_c$, to a decreasing polynomial for $x > x_c$. In the limit $\beta \rightarrow 0$, $x_c \rightarrow 1$, $c(E_\tau) \sim 1$, and the τ rest frame shape is recovered, while for $\beta \rightarrow 1, x_c \rightarrow 0$, and the distribution becomes a smooth decreasing polynomal.

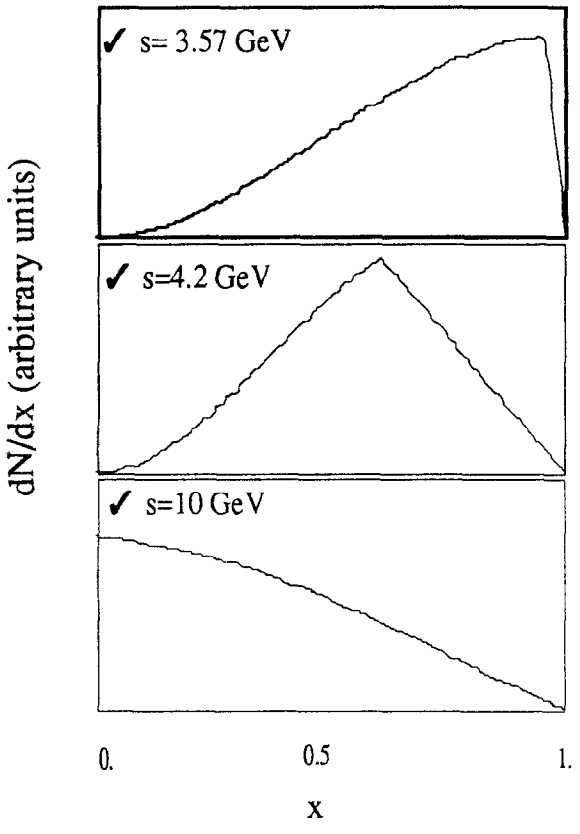

Fig. 18 E_{lepton} for the decay$\tau \rightarrow l\bar{\nu}_l\nu_\tau$ at $\sqrt{s} = 3.57,\ 4.2$, and 10 GeV.

Formula (4.2) can be generalized to take into account the masses of the emitted leptons[24]. In particular, we can estimate the influence of a massive ν_τ in the determination of ρ. To illustrate this point consider the case where the emitted lepton (and its neutrino) is considered as massless but not the τ neutrino (i.e. the decay $\tau \rightarrow e\bar{\nu}_e\nu_\tau$ assuming a massless e and ν_e). In this case we have

$$\frac{dN}{dx} = (\frac{dN}{dx})_{\epsilon=0} + O_1(\epsilon) \quad \text{for } x < x_c \tag{4.3}$$

$$\frac{dN}{dx} = (\frac{dN}{dx})_{\epsilon=0} + O_2(\epsilon) \quad \text{for } x > x_c$$

where

$$O_1(\epsilon) = -2\epsilon(1-\rho) + \frac{2}{3}\sqrt{\epsilon(3\rho - 4\rho^2)}$$

$$O_2(\epsilon) = 2\epsilon[9(x^2-1)+\rho(7-9x^2)] + 6\sqrt{\epsilon(3\rho-4\rho^2)}(1-x^2)$$

and $\epsilon = (\frac{m_{\nu_\tau}}{m_\tau})^2$. As it can be seen the ν_τ mass influence in expression (4.3) is very weak. In particular, for the "V-A" value, $\rho = 3/4$, the dependence on $\sqrt{\epsilon}$ vanishes.

The experimental technique to measure ρ is to obtain the electron (muon) energy spectrum from the τ decay $\tau \rightarrow e\bar{\nu}_e\nu_\tau$ ($\tau \rightarrow \mu\bar{\nu}_\mu\nu_\tau$), then fit this spectrum to the theoretical expression (4.2) (or (4.3) to include the effect of a massive neutrino), corrected to take into account the effect of the radiative corrections (explicit expressions for the radiative corrections to the decay $\tau \rightarrow l\bar{\nu}_l\nu_\tau$ with l=e,μ have been discussed in ref 25 and references therein) and folded with a resolution function describing the detector resolution, acceptance etc, with ρ (or ρ, m_{ν_τ}) as a free parameter.

As was the case for the measurement of the one prong branching fractions, the best place to measure ρ is at threshold where we can "tag" the decays $\tau \rightarrow e\bar{\nu}_e\nu_\tau$ and $\tau \rightarrow \mu\bar{\nu}_\mu\nu_\tau$ with the quasi-monochromatic π produced in the decay $\tau^- \rightarrow \pi^-\nu_\tau$. Furthermore, we only need to separate electrons and muons in practically the whole spectrum, since the π's and K's are spikes of well defined energy. In addition, we will be able to measure the low energy part of the spectrum without being limited by hadronic contamination. In one year run, we can achieve a fractional error on the value of ρ of the order of 0.4 %, comparable with the error obtained in μ decays.

A *B Factory* experiment has several disadvantages compared to the τ – *Charm Factory* to measure ρ. First, at $\sqrt{s} \sim 10\ GeV$ the lepton spectrum is very distorted by the Lorentz Boost, second, particle confusion, especially in the low energy part of the spectrum will probably be a serious problem. A *B Factory* experiment will need a very good understanding of systematic errors that in the case of the τ – *Charm Factory* simply do not exist.

4.2. MEASUREMENT OF ξ AND δ IN THE $\tau - Charm\ Factory$

Consider the decay of a polarized $\tau^-(\epsilon)$

$$\tau^-(\epsilon) \rightarrow \mathrm{a}^- + \nu_\tau + ...$$

Where the particle a with momentum $\mathbf{k_a}$ is detected. Then, the decay distribution of a in the τ rest frame is a function of k_a and $\epsilon \cdot \mathbf{k_a}$.

$$k_a \frac{d\Gamma}{d^3 k_a} = \Gamma \frac{2}{\pi m_\tau^3 \lambda_a} [ka G_1^a(x_a) - \epsilon \mathbf{k_a} \mathrm{G_2^a(x_a)}] \tag{4.4}$$

where we assume a massless. Thus, $x_a = 2k_a/m_\tau$ and

$$\lambda_a = \int dx_a \cdot x_a^2 \cdot G_1^a(x_a).$$

In expression (4.4), G_1^a specifies the spin-independent part of the distribution while G_2^a specifies the spin-dependent part of the distribution. Once G_1 and G_2 are known, the distribution is completely specified. Taking, for example, the leptonic decay $\tau^- \rightarrow \mu^- \nu_\tau \overline{\nu_e}$, we have

$$G_1^\mu = 1 - x + \frac{2}{3}\rho_\mu(\frac{4}{3}x - 1);\ G_2^\mu = A_\mu[1 - x + \frac{2}{3}D_\mu(\frac{4}{3}x - 1)]$$

where

$$\xi_\mu = 3 \cdot A_\mu,\ \delta_\mu = \frac{1}{3}D_\mu$$

Thus, if the τ polarization direction ϵ is known, ξ and δ can be determined directly from the one-particle distribution, fitting the spin dependent part, in the same way that the fit to the spin-independent part gives ρ.

Unfortunately the τ polarization direction is not known in general. However ξ and δ can still be determined due to the fact that the spins of the two τ's produced

in $e^+ e^-$ annihilation are strongly correlated. The procedure is as follows. Consider the process

$$e^+ + e^- \rightarrow \text{"}\gamma\text{"} \rightarrow \tau^+(\epsilon^+)\tau^-(\epsilon^-)$$

$$\tau^+ \rightarrow b^+ + \overline{\nu_\tau} + ...; \quad \tau^- \rightarrow a^- + \nu_\tau + ...$$

Then one can compute the cross section for the production of the particles a and b, in the τ rest frame, performing a coherent sum over the (unobserved) spins of the τ's. This general formula has been computed in ref 26, and 27. They obtain:

$$k_a k_b \frac{d\sigma^{ab}}{d^3k_a d^3k_b d\Omega_\tau} = C[\wp(uncorr) - \wp(corr)] \tag{4.5}$$

where

$$C = \frac{\alpha^2\beta}{4\pi^2 E_\tau^2 m_\tau^6 \lambda_a \lambda_b}$$

and $\wp(uncorr)$, $\wp(corr)$ are respectively the spin-uncorrelated and spin-correlated parts of the distribution.

$$\wp(uncorr) = G_1^a(x_a) \cdot G_1^b(x_b) \cdot f_1(\theta_\tau, k_a, k_b)$$

$$\wp(corr) = G_2^a(x_a) \cdot G_2^b(x_b) \cdot f_2(\theta_\tau, k_a, k_b)$$

The functions f_1 and f_2 are given explicitly in Reference 26.

The distributions that are relevant to experiments can be calculated from expresion (4.5), integrating over the unobserved variables

$$\frac{d\sigma}{dr_1...dr_n} = \int k_a k_b \frac{d\sigma^{ab}}{d^3k_a d^3k_b d\Omega_\tau} \prod_{i=1}^{n} \delta(r_i - r_i(\mathbf{k_a}, \mathbf{k_b}, \Omega_\tau)) \mathrm{d}^3\mathrm{k_a} \mathrm{d}^3\mathrm{k_b} \mathrm{d}\Omega_\tau \tag{4.6}$$

where $r_i(\mathbf{k_a}, \mathbf{k_b}, \Omega_\tau)$ are the Laboratory variables r_i expressed in terms of $\mathbf{k_a}, \mathbf{k_b}$ and Ω_τ.

In general, the integral in equation (4.6) must be computed numerically. However in a few simple cases, analytical expressions can be found. In particular, since the TCF experiment will be able to take data close to the τ pair production threshold, we can compute the limit for equation (4.5) when $\gamma \rightarrow 1$ and obtain a simple formula for the cross section

$$\frac{dN}{dx_a dx_b d\Omega_a d\Omega_b} = N_0 \cdot F_{th} \tag{4.7}$$

where

$$F_{th} = G_1^a(x_a)G_1^b(x_b) - G_2^a(x_a)G_2^b(x_b)\cos\theta_a \cos\theta_b$$

The spin dependent part in equation (4.7) vanishes when integrating over the solid angle. That is, near threshold the energy correlation $\frac{dN}{dx_a dx_b}$ does not contain any information on the τ spin structure, and simply factorizes into the one-particle distributions.

$$\frac{dN}{dx_a dx_b} = \frac{dN}{dx_a} \cdot \frac{dN}{dx_b}. \tag{4.8}$$

However, the angular correlation gives information on the spin-dependent part of the distribution. Taking the particles a and b to be $a = l(e,\mu), b = \pi$ we obtain:

$$\frac{dN}{d\cos\theta_l \cos\theta_\pi} = N_0[1 - \frac{1}{3}\xi_l h_{\nu_\tau} \cos\theta_l cos\theta_\pi] \tag{4.9}$$

where h_{ν_τ} is the helicity of the τ neutrino. Taking a=e, b=μ we obtain

$$\frac{dN}{d\cos\theta_e \cos\theta_\mu} = N_0[1 - \frac{1}{9}\xi_e\xi_\mu \cos\theta_e cos\theta_\mu] \tag{4.10}$$

Thus, one possiblity for measuring ξ_e, ξ_μ, and h_{ν_τ} is to compute the angular correlations for the processes $\tau \rightarrow l\bar{\nu}_l\nu_\tau$ (l=e,μ), $\tau^+ \rightarrow \pi^+\nu_\tau$ and $\tau \rightarrow e\bar{\nu}_e\nu_\tau$, $\tau^+ \rightarrow \mu^+\bar{\nu}_\mu\nu_\tau$, and fit them to equations (4.9), (4.10). The fit gives $\xi_e h_{\nu_\tau}$, $\xi_\mu h_{\nu_\tau}$ and ξ_e, ξ_μ, from where we obtain the absolute value of ξ_e, ξ_μ and h_{ν_τ}. The sign of the τ neutrino helicity can be measured in a separate experiment (see ref 28). This fixes in turn the sign of ξ_e, ξ_μ.

At low energy (near threshold) we do not measure δ_e, δ_μ. This measurement has to be done at higher energies, (i.e. at $\sqrt{s} = 4.2\ GeV$) where the energy correlation is significant. At this energy, ξ_e, ξ_μ, δ_e and δ_μ can be measured from the energy correlations between the e,μ and π distributions. The energy correlation between two particles a and b can be obtained from equation (4.6). In this case the integral over the unobserved variables can be computed analytically. We obtain:

$$\frac{dN}{dx_a dx_b} = N_0[F_{uncorr} + F_{corr}] \tag{4.11}$$

As above, we now take

$$a = l(e,\mu)\ b = \pi :$$

$$F_{uncorr} = k_2(x_l, \rho_l); \quad F_{corr} = \varpi(\beta,\gamma) \cdot \xi_l \cdot h_{\nu_\tau} \cdot \varphi(x_\pi) \cdot \varphi(x_l)$$

and

$$a = e,\ b = \mu :$$

$$F_{uncorr} = k_2(x_e, \rho_e) \cdot k_2(x_\mu, \rho_\mu); \quad F_{corr} = \varpi(\beta,\gamma) \cdot \xi_e \cdot \xi_\mu \cdot \varphi(x_\mu) \cdot \varphi(x_e)$$

where

$$\varpi(\beta,\gamma) = \frac{1}{2\beta^2} \cdot \frac{2\gamma^2 - 1}{2\gamma^2 + 1},$$

$$\varphi(x_l) = k_2(x_l, \delta_l) - (1+\beta)x_l \cdot k_1(x_l, \delta_l)$$

and

$$\varphi(x_\pi) = 1 - (1+\beta)x_\pi.$$

The functions K_n are defined by:

$$K_n(x,\delta) = A_n(x) - A_{n+1}(x) + \frac{2}{3}\delta[\frac{4}{3}A_{n+1}(x) - A_n(x)]$$

where

$$A_n(x) = \frac{1}{n}[(\frac{1}{x_c})^n - 1]x^n, \quad x < x_c,$$

$$A_n(x) = \frac{1}{n}[1 - x^n], \quad x > x_c.$$

In the limit $\gamma \to 1, \varphi(x_l) \to 0$ and thus $F_{corr} \to 0$ as we had obtained before. However, at $\sqrt{s} = 4.2\ GeV$, the energy correlation is already significant. To illustrate this point, in Figure 19, we show the 1-dimensional projection of F_{corr} and F_{uncorr} at three different energies, $\sqrt{s} = 3.57$, 4.2 and 10 GeV ($\beta = 0.03$, 0.5 and 0.9). Notice that while at $\sqrt{s} = 3.57$ $F_{corr} \to 0$, the influence of F_{corr} is similar at $\sqrt{s} = 4.5\ GeV$ and $\sqrt{s} = 10\ GeV$, about a 10% effect in a substantial region of phase space.

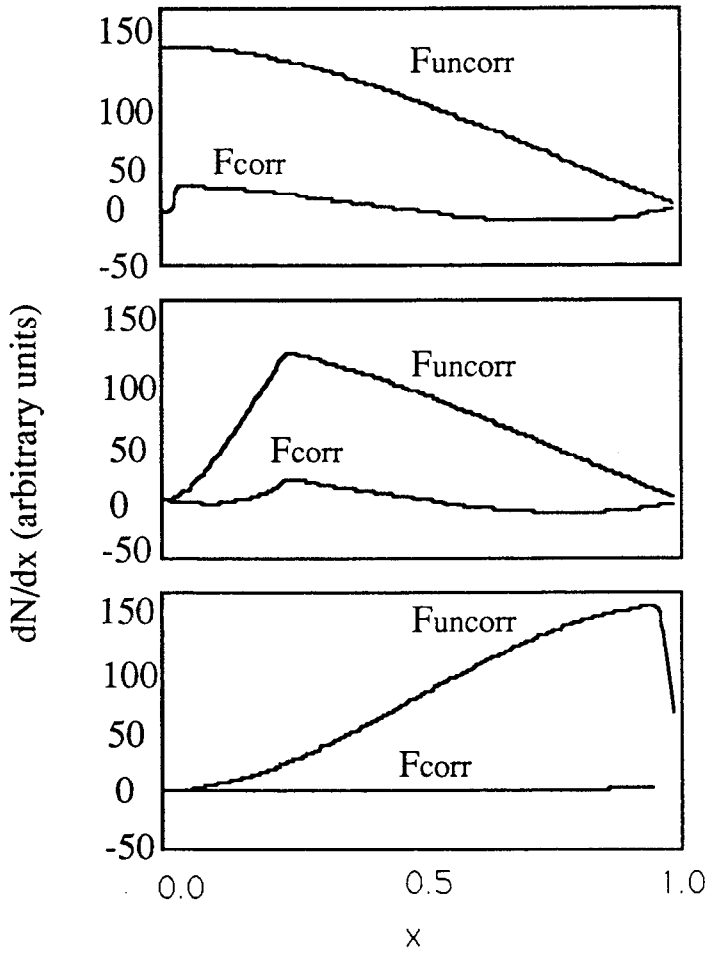

Fig. 19 1-dimensional projection of F_{corr} and F_{uncorr} at $\sqrt{s} = 3.57, 4.2$ and 10 GeV.

Thus, we can measure ξ_e, ξ_μ, δ_e and δ_μ by fitting equation (4.11)to the energy correlations for the processes $\tau \to l\bar{\nu}_l\nu_\tau$ (l=e,μ), $\tau^+ \to \pi^+\nu_\tau$. In a year run we obtain a precision of the order of 1 % for these parameters. This measurement can be performed with about the same precision by a *B Factory* experiment. This has been extensively studied by Fetscher.[28,21]

4.3. Measurement of ξ'

The longitudinal polarization of the lepton emitted in the τ decay, averaged over its energy and emission angle, is equal to ξ'.[29] It has been pointed out[28], that ξ'_μ can be measured using μ decay as an analyzer of the μ polarization. The technique is as follows. The μ produced via the decay $\tau \to \mu\bar{\nu}_\mu\nu_\tau$ must be stopped in a "polarimeter" (that is a detector able to stop the μ with minimum depolarization, and to detect the emitted electrons from μ decay) where they decay in a weak magnetic field, $B \sim 60$ G. The longitudinal projection of the spin of a stopping μ precesses in the polarimeter with a frequency induced by the magnetic field ω in a plane perpendicular to that field. Because of the well established $V-A$ interaction in muon decay, the daughter electrons are emitted preferently in the direction of the muon spin. It is therefore, expected to observe a time dependent forward-backward asymmetry on the electron distribution.

$$R(t) = \frac{N_B(t) - N_F(t)}{N_B(t) + N_F(t)} = R_0 \cos(\omega t + \phi)$$

The phase ϕ is expected to be $\phi = 0$ for negative helicity and $\phi = -\pi$ for positive helicity. The oscillation amplitude R_0 is proportional to the magnitude of longitudinal polarization ξ'_μ and the polarimeter analysing power α.

$$R_0 = \alpha \cdot \xi'_\mu$$

The experimental problem is how to incorporate such a polarimeter in a τ – *Charm Factory* experiment. Several alternatives are possible, such as using a fine

grane sandwich hadronic calorimeter with low depolarization material, or build a separate detector after the hadronic calorimeter.

.5. Summary

We have discussed some of the most important τ physics experiments that can be carried out by the proposed $\tau - Charm\ Factory$. The impressive results projected for the sensitivity to a massive τ neutrino , the measurement of the one-prong branching fractions and the determination of the Michel parameters are possible due not only to the very high τ pair production rates and excellent detector, but, because of the ability of taking data at low energy. This last point is of enormous importance. It will allow a very precise measurement of the branching fractions for the processes $\tau \rightarrow e\bar{\nu}_e\nu_\tau, \tau \rightarrow \mu\bar{\nu}_\mu\nu_\tau, \tau^- \rightarrow \pi^-\nu_\tau$, $\tau^- \rightarrow K^-\nu_\tau$, and the Michel parameter ρ, where one uses the kinematical separation that τ pair production at threshold provides. Low energy τ's permit a very good mass resolution, necessary for the study of the limits on m_{ν_τ}. This last experiment can be performed either above or below Charm production threshold. One can also take data below τ pairs production threshold in order to measure the hadronic backgrounds.

To summarize, there is a very beautiful τ physics yet to be studied. And the best place to do it, is in the low energy sector, near the τ and charm production threshold. That is, in the Charm Land.

Acknowledgements:

For this study I have worked very closely with Abe Seiden. This has been a terrific,funny and very instructive experience. I have enjoyed many interesting discussions with Pat Burchat, Concha Gonzalez, Eloina Maestro, Toni Pich and Rafe Schindler. Finally, I want to acknowledge the Fulbright Grant that has supported my work for the last two years.

REFERENCES

1. M.L. Perl et al., Phys. Rev. Lett. **35,1489** (1975).
2. J. Kirkby this proceedings.
3. A. Seiden, this proceedings.
4. H. Albercht et al., Phys.Lett. **202 B** (1988)149.
5. M. Frischi et al., Phys.Lett. **173 B** (1986) 485.
6. R. Abela et al., Phys.Lett. **146 B** (1984)431.
7. R.R. Mendel et al., Z Phys. **C 32** (1986)517.
8. J.J. Gomez-Cadenas and M.C. Gonzalez-Garcia, Phys.Rev. **D 39** (1989)1370.
9. J.J. Gomez-Cadenas et al. SCIPP 88/32 (1989); Phys.ReV.D, to be published.
10. M.C. Gonzalez-Garcia et al. SCIPP preprint, to be published.
11. M. Voloshin, this proceedings.
12. A. Pich et al., CERN-TH-5185/88, Sep. 1988.
13. G.B. Mills et al. (Delco Collaboration) Phys. Rev. Lett. **54** (1985)624.
14. F.Gilman and S.H. Rhie, Phys. Rev. **31**,1066(1985).
15. W.J. Marciano and A. Sirlin, Phys. Rev. Lett. **61**,1815(1988).
16. J.J. Gomez-Cadenas, C.A. Heusch, and A. Seiden. SCIPP 89/29. Particle World, to be published.
17. C.A. Heusch, SCIPP 89/21 May, 1989).
18. A. Pich and S. Narison, Phys. Lett. **211 B**(1988)183.
19. E. Braaten, Phys. Rev. Lett. **60**(1988)1606.
20. W. Fetscher, 12th International Conference on Neutrino Physics and Astrophysics, Sendai, Japan, June 1986.

21. See contributions by W. Fetscher and by Y.Y. Tsai, this proceedings.

22. H.J. Gerber, Lepton Properties, International Europhysics Conference on High Energy Physics, Uppsale (Sweden),1987.

23. Y.S. Tsai., SLAC-PUB-5029, SLAC-PUB-5003, May (1989).

24. J.J. Gomez-Cadenas et al. SCIPP 89/09. Phys Rev. D. to be published.

25. A. Ali and Z. Z. Aydin, Nuovo Cimento, **43 A**(1978)270.

26. S.Y. Pi and A.I. Sanda. Annals of Physics **106**(1977)171.

27. Y.S. Tsai Phys Rev **D4** (1971)2821.

28. W. Fetscher, Leptonic τ decays. Proceedings of the SIN factory Workshop.

29. F. Scheck, Phys. Rep. 44(1978).

FIGURE CAPTIONS

1) The shape of the electron energy distribution for different m_{ν_τ}, close to the end-point, for a τ decaying at rest

2) Hadronic mass distributions for the decay $\tau^- \rightarrow K^-K^+\pi^-\nu_\tau$. Solid line is our model for the decay. Dashed line is pure 3-body phase space. The normalization of both distributions is the same

3) Hadronic mass distributions for the decay $\tau^- \rightarrow K^-K^+\pi^-\nu_\tau$ in the range $m_{had} > 1750$ MeV. The dashed line is the model prediction. The dotted line is pure 3-body phase space. The normalization of both distributions is the same

4) (a) Electron energy distribution. (b) Inclusive momentum for the hadrons.

5) (a) Missing momentum and (b) Missing energy for the decay $\tau^- \rightarrow K^-K^+\pi^-\nu_\tau$ tagged by $\tau \rightarrow e\bar{\nu}_e\nu_\tau$

6) Hadronic mass distribution for the decay $\tau^- \rightarrow \rho^0\rho^0\pi^-\nu_\tau$ with the ρ's subsequetly decaying into charged pions. The dots are Argus data

7) The lepton momentum spectrum for the signal (the tag taken to be$\tau \rightarrow e\bar{\nu}_e\nu_\tau$) and the hadronic background.

8) Missing momentum (a) and Reduced mass (b) for the signal and the background.

9) Hadronic mass for the signal and the background

10) Hadronic mass distribution for different m_{ν_τ}, togheter with the best fits to them

11) Inclusive momentum distribution for the decay $\tau^- \rightarrow \pi^-\pi^+\pi^-\pi^+\pi^-\nu_\tau$ at 4.2 (solid line) and 10 GeV (dotted) center of mass energy

12) The τ cross section as a function of the center-of-mass energy

13) Momentum spectra for the τ decays to e,μ, π and K at threshold ($E_\tau = 1.785\ GeV$.

14) Momentum spectra for the τ decays to e,μ, π, and K at the τ–$Charm\ Factory$ maximum energy ($E_\tau = 2.25\ GeV$.

15) Missing energy for the signal and the hadronic background

16) The signal and the hadronic backgrounds after the selection cuts

17) The energy spectrum of the emitted lepton in the decay $\tau \rightarrow l\bar{\nu}_l\nu_\tau$. in the τ rest frame. (a) $\rho = 3/4$ ("V-A"); (b) $\rho = 0$ ("V+A").

18) The energy spectrum of the emitted lepton in the decay $\tau \rightarrow l\bar{\nu}_l\nu_\tau$. in the Laboratory frame, for $\rho = 3/4$ and different center of mass energies. (a) $\sqrt{s} = 3.57\ GeV$ (b) $\sqrt{s} = 3.68\ GeV$ (c) $\sqrt{s} = 10.0\ GeV$.

19) 1-dimensional projection of F_{corr} and F_{uncorr} at different center of mass energies. (a) At threshold ($\sqrt{s} = 3.569\ GeV$) (b) At TCF maximum energy ($\sqrt{s} = 4.500\ GeV$) (c) At BF running energy ($\sqrt{s} = 10.00\ GeV$)